



Influence of different arylamine electron donors in organic sensitizers for dye-sensitized solar cells

Zhongquan Wan^a, Chunyang Jia^{a,*}, Linlei Zhou^a, Weirong Huo^a, Xiaojun Yao^b, Yu Shi^a

^a State Key Laboratory of Electronic Thin Films and Integrated Devices, School of Microelectronics and Solid-State Electronics, University of Electronic Science and Technology of China, Chengdu 610054, PR China

^b State Key Laboratory of Applied Organic Chemistry, School of Chemistry and Chemical Engineering, Lanzhou University, Lanzhou 730000, PR China

ARTICLE INFO

Article history:

Received 21 February 2012

Received in revised form

23 March 2012

Accepted 23 March 2012

Available online 31 March 2012

Keywords:

Dye-sensitized solar cells

Electron donor

Carbazole

Phenothiazine

Diphenylamine

Electrochemical impedance spectroscopy

ABSTRACT

Three organic sensitizers containing identical π -spacers and electron acceptors but different arylamine electron donors, carbazole, phenothiazine and diphenylamine, were applied in dye-sensitized solar cells to study the influence of the different electron donors on the photophysical, electrochemical and photovoltaic properties by spectral, electrochemical, photovoltaic experiments, and density functional theory calculations. The overall dye-sensitized solar cell conversion efficiencies ranged from 1.77% to 2.03%. Electrochemical impedance spectroscopy results are in good agreement with results of the short-circuit currents and the overall conversion efficiencies of the dye-sensitized solar cells based on the three dyes.

© 2012 Elsevier Ltd. All rights reserved.

1. Introduction

As petroleum and coal are depleted, renewable energy sources have attracted increasing attention, and solar energy is considered as a good alternate for fossil fuel energy. Therefore, dye-sensitized solar cells (DSSCs) have attracted more and more attention in recent years due to their potential advantages of low cost, ease of production, flexibility, and transparency relative to conventional crystalline silicon solar cells.

In DSSCs, the dye is one of the most important components influencing the performance of solar cell, because the choice of dye determines the photoresponse of the DSSCs and initiates the primary steps of photon absorption and the subsequent electron transfer process. DSSCs based on the ruthenium sensitizers have shown very impressive overall conversion efficiencies, reaching 11% under standard AM 1.5G sunlight [1]. However, the large-scale application of ruthenium dyes is limited because of costs and environmental issues. More and more efforts have been dedicated to the development of metal-free organic dyes which exhibit not

only higher molar extinction coefficients, but also simple preparation and purification procedures at lower cost.

Many metal-free organic dyes have been used in DSSCs, such as, coumarin [2], merocyanine [3], indoline [4,5], polyene [6], hemicyanine [7], triphenylamine [8], fluorene [9], carbazole [10] and phenothiazine [11–13] based-organic dyes. Generally, metal-free organic dyes possess the evident molecular structure of the electron donor part and the acceptor part bridged by the conjugated chain (D– π –A). In this structure, small variations within these different sections cause significant differences in photovoltaic properties [14–16].

Because the electron donors in organic sensitizers play a crucial role in determining the overall conversion efficiency, a series of organic sensitizers containing identical π -spacers (benzene) and electron acceptors (cyanoacetic acid) but different arylamine electron donors (carbazole for **CBZ**, phenothiazine for **WD-5**, diphenylamine for **DTA**) were applied in DSSCs to study the influence of the different arylamine electron donors on the photophysical, electrochemical properties and photovoltaic performances by spectral, electrochemical, photovoltaic experiments, and density functional theory calculations. The corresponding molecular structures of the three dyes are shown in Fig. 1.

* Corresponding author. Tel.: +86 2883202550; fax: +86 2883202569.

E-mail address: cjia@uestc.edu.cn (C. Jia).

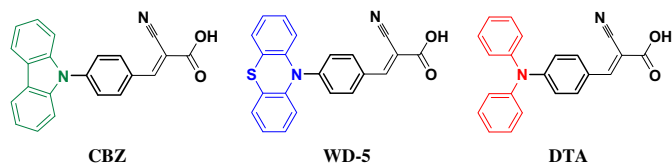


Fig. 1. Molecular structures of **CBZ**, **WD-5** and **DTA**.

2. Experimental section

2.1. Materials and characterization

All solvents and other chemicals were reagent grade and used without further purification. The electrolyte consisted of 0.6 M 1,2-dimethyl-3-propylimidazolium iodide (DMPII), 0.025 M LiI, 0.04 M I₂, 0.05 M guanidium thiocyanate (GuSCN), and 0.28 M 4-tertbutylpyridine (TBP) in dry acetonitrile was purchased from Heptachroma. Cyanoacetic acid was purchased from Aldrich. Carbazole, phenothiazine and diphenylamine were purchased from Astatech. The melting points were taken on X-4 melting point apparatus. ¹H NMR and ¹³C NMR spectra were recorded on Bruker AVANCE III 400 MHz. TOF-MS spectra were determined with a BEFLEX III spectrometer. HRMS data were determined with an FTICR-APEX instrument.

2.2. Photophysical and electrochemical measurements

Absorption spectra were measured with SHIMADZU (model UV1700) UV–Vis spectrophotometer. Cyclic voltammetry experiments were performed on a CH Instruments 660C electrochemical workstation at a scan rate of 100 mV/s in CH₂Cl₂ (5.2×10^{-4} mol/L) containing 0.1 mol/L *n*-Bu₄NPF₆ as the supporting electrolyte, platinum as counter and work electrodes and Ag/AgCl as reference electrode.

2.3. Synthesis

CBZ and **DTA** dyes were synthesized according to the literature [17]. The synthetic route of **WD-5** is shown in Fig. 2.

2.3.1. Compound 2

Phenothiazine (0.12 g, 0.603 mmol), 4-bromobenzaldehyde (0.17 g, 0.913 mmol), potassium carbonate (0.35 g, 2.536 mmol), activated copper bronze (0.093 g, 1.463 mmol) and 18-crown-6 (0.016 g, 0.061 mmol) were heated under reflux in 1,2-dichlorobenzene (20 mL) for 48 h. The mixture was filtered and the product purified by column chromatography using toluene as the eluent, which gave the compound **2** as a green glass. Yield: 59%. Mp: 90–92 °C. MALDI-TOF (*m/z*): calcd for C₁₉H₁₃NOS: 303.1, found 303.1 [M]⁺. HRMS-EI (*m/z*): calcd for C₁₉H₁₃NOS, 303.0718; found, 303.0752.

2.3.2. **WD-5**

Compound **2** (0.091 g, 0.3 mmol), cyanoacetic acid (0.038 g, 0.45 mmol), and piperidine (2.0 mmol) were added to chloroform

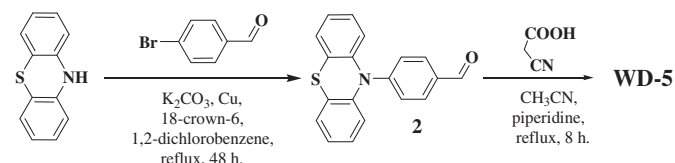


Fig. 2. Synthetic route of the dye **WD-5**.

(20 mL) and the mixture was heated under reflux for 8 h. After that water (20 mL) was added to the reaction mixture. The solution was acidified with 20% aqueous HCl (30 mL) and extracted with chloroform. The organic phase was dried over anhydrous sodium sulfate. The solvent was evaporated on a rotaevaporator under vacuum and the residue was purified on a column chromatography with dichloromethane/methanol as eluent to give the crude product. The crude product was dissolved in chloroform, and washed with an HCl aqueous solution. The remove of solvent under reduced pressure gives the final dye **WD-5** as a dark yellow solid. Yield: 68%. Mp: 145–147 °C. ¹H NMR (400 MHz, acetone-*d*₆, ppm): δ 6.92–6.89 (t, *J* = 12.0 Hz, 2H), 7.10–7.08 (d, *J* = 8.0 Hz, 2H), 7.23 (t, *J* = 12.0 Hz, 2H), 7.43–7.42 (d, *J* = 4.0 Hz, 2H), 8.05 (t, *J* = 8.0 Hz, 2H), 8.15 (s, 1H), 8.17 (s, 1H), 8.22 (s, 1H). ¹³C NMR (100 MHz, acetone-*d*₆, ppm): δ 169.57, 155.08, 155.01, 150.86, 142.49, 134.63, 133.99, 128.25, 124.58, 118.77, 118.17, 101.95, 100.15, 55.53. MALDI-TOF (*m/z*): calcd for C₂₂H₁₄N₂O₂S: 370.1, found 369.1 [M–H]⁺. HRMS-EI (*m/z*): calcd for C₂₂H₁₄N₂O₂S, 370.0776; found, 370.0768.

2.4. Theoretical calculations

Gaussian 03 package was used for density functional theory (DFT) calculations [18]. The geometries and energies of the three dyes were determined using the B3LYP method with the 6–31G (d,p) basis set. Importantly, none of the frequency calculations generated negative frequencies, being consistent with an energy minimum for the optimized geometry.

2.5. Fabrication of dye-sensitized solar cells

A layer of approximately 2 μm TiO₂ (13 nm paste, DHS-TPP3, Heptachroma, China) was coated on the F-doped tin oxide conducting glass (TEC15, 15 Ω per square, Pilkington, USA) by screen printing and then dried for 6 min at 125 °C. This procedure was repeated 6 times (around 12 μm) and finally coated by a layer (around 4 μm) of TiO₂ paste (200 nm paste, DHS-TPP200, Heptachroma, China) as scattering layer. The double-layer TiO₂ electrodes (area: 6 × 6 mm) were gradually heated under an air flow at 325 °C for 5 min, at 375 °C for 5 min, at 450 °C for 15 min, and at 500 °C for 15 min. The sintered film was further treated with 40 mm TiCl₄ aqueous solution at 70 °C for 30 min, then washed with ethanol and water, and annealed at 500 °C for 30 min. After the film was cooled to 40 °C, it was immersed into a 0.2 mM dye bath in CH₂Cl₂ solution and maintained in the dark for 12 h. The electrode was then rinsed with CH₂Cl₂ and dried. In our experiment, open cells were fabricated in air by clamping the different dyed electrodes with platinized counter electrode. The electrolyte consisted of 0.6 M 1,2-dimethyl-3-propylimidazolium iodide (DMPII), 0.025 M LiI, 0.04 M I₂, 0.05 M guanidium thiocyanate (GuSCN), and 0.28 M 4-tertbutylpyridine (TBP) in dry acetonitrile.

2.6. Photovoltaic characterization

The irradiation source for the photocurrent–voltage (*J*–*V*) measurement is a xenon lamp (CHF-XM-500W, Trustech Co. Ltd., Beijing, China). The incident light intensity was 100 mW cm^{−2} calibrated with a standard Si solar cell. The current–voltage curves were obtained by linear sweep voltammetry (LSV) method using a CHI660C electrochemistry workstation (Shanghai CH Instruments Co., China). The spectra of monochromatic incident photon-to-current conversion efficiency (IPCE) for solar cells were performed by using a commercial setup (QTest Station 2000 IPCE Measurement System, CROWNTech, USA). The electrochemical impedance spectra (EIS) measurements were carried out by applying bias of the open-circuit voltage (*V*_{oc}) and recorded over a frequency range of

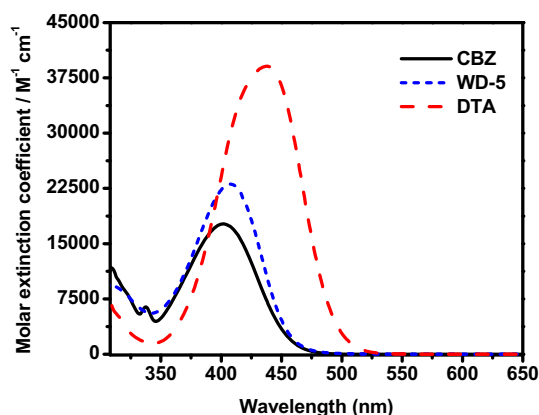


Fig. 3. Absorption spectra of CBZ, WD-5 and DTA recorded in dichloromethane.

0.1 Hz–100 kHz with AC amplitude of 10 mV. The measurement was carried out on a CHI660C electrochemical analyzer (CH Instruments) combined with Xe lamp as the light source.

3. Results and discussion

3.1. Optical properties

The influence of different arylamine electron donors on the light harvest capacity of a dye molecule was first evaluated by recording the UV–vis absorption spectra of the dyes dissolved in dichloromethane (Fig. 3), and the selected parameters were collected in Table 1.

CBZ, WD-5 and DTA showed the maximum absorption wavelength (λ_{\max}) 401 nm (molar absorption coefficient (ϵ) = 17,690 M⁻¹ cm⁻¹), 408 nm (ϵ = 23,083 M⁻¹ cm⁻¹) and 438 nm (ϵ = 39,085 M⁻¹ cm⁻¹), respectively, which were corresponding to HOMO (highest occupied molecular orbital) → LUMO (lowest unoccupied molecular orbital) transition. Amongst these photosensitizers, due to strong electron donating ability of the diphenylamine unit, the DTA dye with the diphenylamine electron donor presents the longest maximum absorption wavelength, with the highest molar absorption coefficient, which is an advantageous spectral property for light harvesting of the solar spectrum.

Fig. 4 shows the absorption spectra of CBZ, WD-5 and DTA on the TiO₂ films after 12 h adsorption. Upon dye adsorption onto the TiO₂ surface, the maximum absorption respectively red-shifted by 38, 41 and 22 nm for CBZ, WD-5 and DTA as compared to the spectra in solution. The broadening of the dyes adsorption on the surface of the TiO₂ films and red shift of the peak maxima is believed to result from the formation of partial J-aggregates [19].

Table 1
UV–vis and electrochemical data.

Dye	λ_{\max}^a /nm (ϵ^b /M ⁻¹ cm ⁻¹)	λ_{\max}^c /nm	E_{ox}^d /V (vs. NHE)	E_g^e /eV	E_{ox}^f /V (vs. NHE)
CBZ	401 (17,690)	439	1.06	2.82	-1.76
WD-5	408 (23,083)	449	1.05	2.80	-1.75
DTA	438 (39,085)	460	1.14	2.60	-1.46

^a Absorption is measured in dichloromethane solutions (2.0 × 10⁻⁵ M) at room temperature.

^b The molar extinction coefficient at λ_{\max} of the absorption spectra.

^c Absorption spectra of the dyes adsorbed on TiO₂ electrodes.

^d E_{ox} was measured in dichloromethane with 0.1 M *n*-Bu₄NPF₆ as electrolyte (scanning rate: 100 mV s⁻¹, working electrode and counter electrode: Pt wires, and reference electrode: Ag/AgCl), potentials measured vs Ag/AgCl were converted to normal hydrogen electrode (NHE) by addition of +0.2 V.

^e E_g was estimated from the absorption spectra of the dyes.

^f E_{ox}^* was calculated from $E_{\text{ox}} - E_g$.

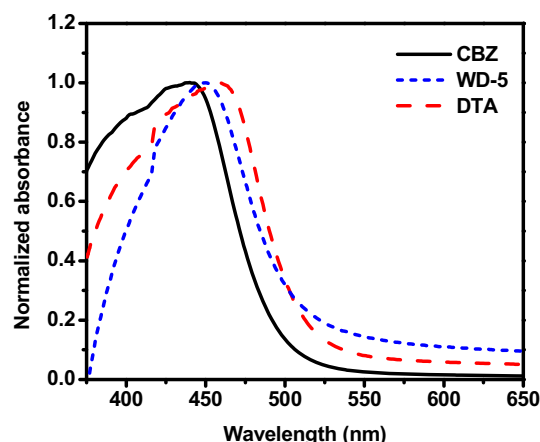


Fig. 4. Absorption spectra of TiO₂ films sensitized by CBZ, WD-5 and DTA.

Furthermore, based on the Tauc relation, the energy gap (E_g) can be obtained by plotting $(ah\nu)^2$ vs. $h\nu$ and extrapolating the linear portion of $(ah\nu)^2$ to zero as shown in Fig. 5 [20]. The E_g of CBZ, WD-5 and DTA are estimated to be 2.82, 2.80 and 2.60 eV, respectively.

3.2. Electrochemical properties

The energetic alignment of the HOMO and LUMO energy levels is crucial for an efficient operation of the dye in DSSCs. To ensure

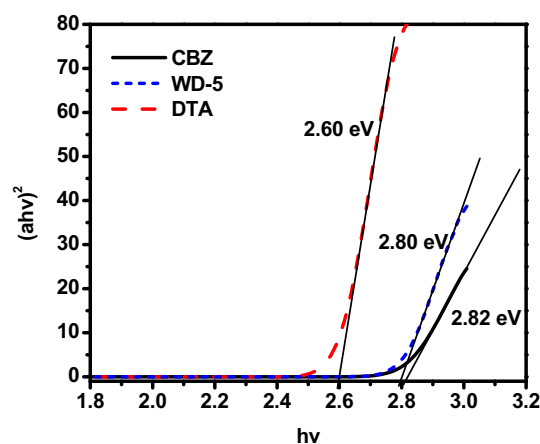


Fig. 5. Plots of $(ah\nu)^2$ vs. $h\nu$.

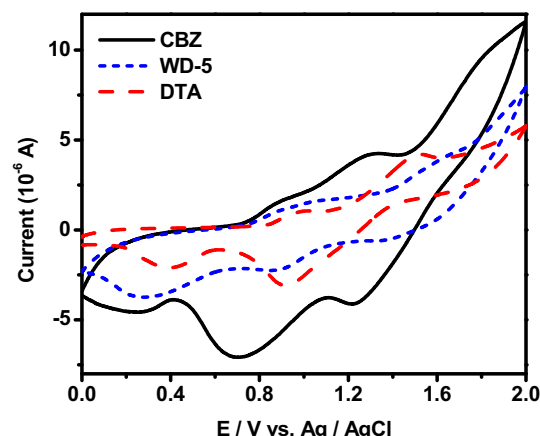


Fig. 6. The CV curves of CBZ, WD-5 and DTA in dichloromethane.

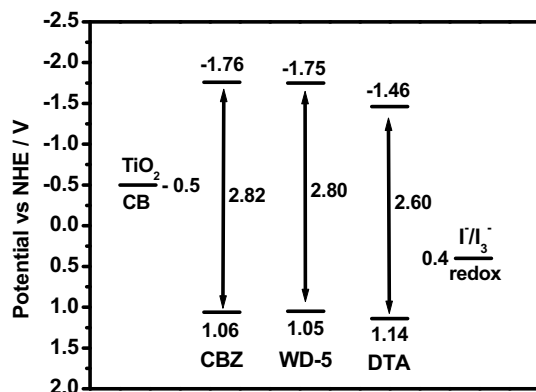


Fig. 7. Schematic energy levels of **CBZ**, **WD-5** and **DTA** based on absorption and electrochemical data.

efficient electron injection from the excited dye into the conduction band of TiO_2 , the LUMO level must be higher in energy than the TiO_2 conduction band edge. The HOMO level of the dye must be lower in energy than the redox potential of the I^-/I_3^- redox couple for efficient regeneration of the dye cation after photoinduced electron injection into the TiO_2 film. To study the influence of the different arylamine electron donors on the energy levels of the dyes, cyclic voltammetry of the three dyes were performed.

As shown in Fig. 6 and Table 1, the first oxidation potentials (E_{ox}) correspond to the HOMO levels of the dyes (**CBZ**: 1.06 V vs NHE; **WD-5**: 1.05 V vs NHE; **DTA**: 1.14 V vs NHE) are more positive than the I^-/I_3^- redox potential (~ 0.4 V vs NHE), providing a thermodynamic driving force for efficient dye regeneration. On the other hand, the excited state oxidation potentials (E_{ox}^*), which

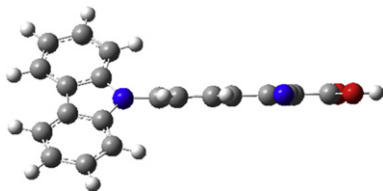
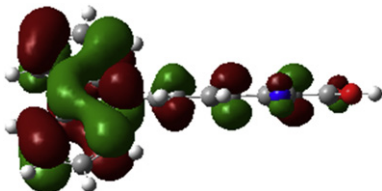
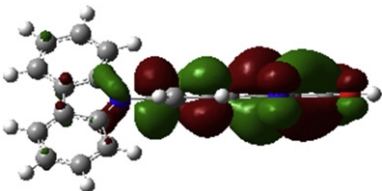
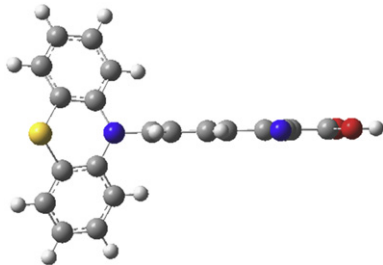
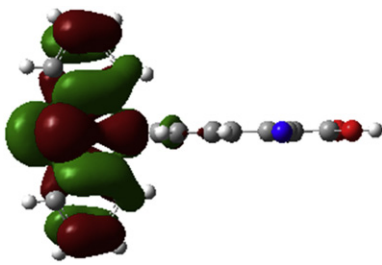
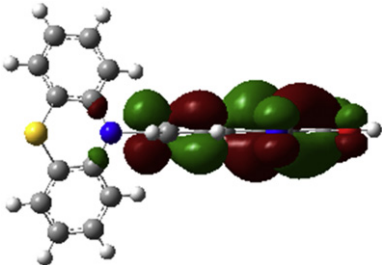
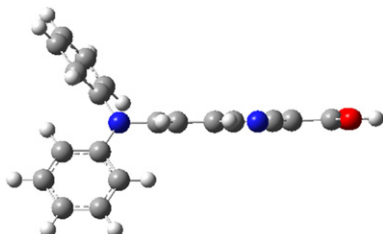
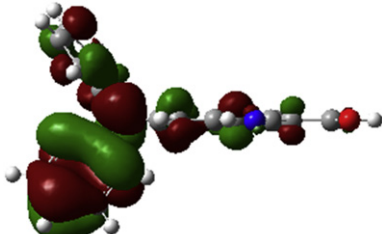
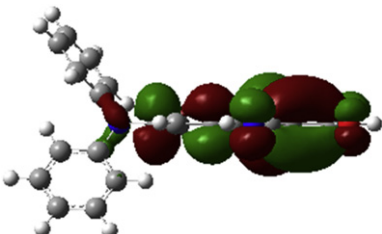
correspond to the LUMO, can be obtained by the E_{ox} and E_g of the dyes, namely, $E_{\text{ox}} - E_g$. The LUMO of three dyes (**CBZ**: -1.76 V; **WD-5**: -1.75 V; **DTA**: -1.46 V vs. NHE) are more negative than the conduction band of TiO_2 (at approximately -0.5 V vs NHE) [21], indicating that the electron injection process from the excited dye molecule to TiO_2 conduction band is energetically favorable. It is worth noting that the HOMO energy level of **DTA** is more positive than the conduction band of TiO_2 relative to **CBZ** and **WD-5**, indicative of the more significant driving force for the reduction of the oxidized dye. These findings denote that the diphenylamine donor in **DTA** dye could enhance the driving force for the reduction of the oxidized dye, thus making the device performance of **DTA** superior to that of **CBZ** and **WD-5**. The schematic energy levels of **CBZ**, **WD-5** and **DTA** based on absorption and electrochemical data are shown in Fig. 7.

3.3. Theoretical calculations

To get further insight into the effect of molecular structures and electron distributions of the three dyes on the performances of DSSCs, their geometries and energies were optimized by density functional theory (DFT) calculations.

According to the optimized dye structures (Table 2), the molecular structure of **CBZ** is prone to aggregation on TiO_2 . The electron donor section of **DTA** exhibits a propeller form and the substituted PTZ framework of **WD-5** is a T type structure. The HOMO is mainly located on the electron donating group and π -spacer, and the LUMO is mainly located in electron withdrawing groups through the π -spacer. It reveals that the benzene π -spacer is essentially coplanar with cyanoacetic acid group. There are effective electron separations between HOMO and LUMO of these dyes induced by light irradiation.

Table 2
The optimized structures and HOMO and LUMO electron distributions of **CBZ**, **WD-5** and **DTA** dyes.

Dye	Optimized structure	HOMO	LUMO
CBZ			
WD-5			
DTA			

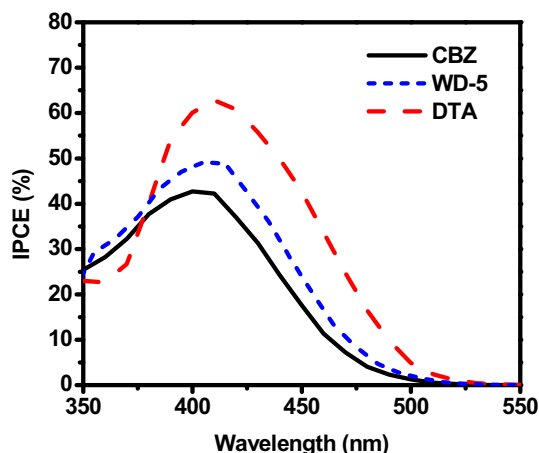


Fig. 8. The IPCE spectra of DSSCs based on **CBZ**, **WD-5** and **DTA** dyes.

3.4. Photovoltaic properties

The incident photon-to-current conversion efficiency (IPCE) of DSSCs based on these dyes is measured, as shown in Fig. 8. The IPCE curves of DSSCs based on **CBZ**, **WD-5** and **DTA** exhibit broad absorption in the range of 350–520 nm, with maxima at 42.7, 49.2, and 62.7% respectively. In comparison with **CBZ** and **WD-5**, **DTA** gives the higher IPCE value, which implies the dye would show a relatively large photocurrent in DSSCs. The higher IPCE value of **DTA** might attribute to the higher molar extinction coefficient. These results are consistent with the absorption spectra in solutions and on TiO_2 films of the dyes.

Fig. 9 shows the J – V curves of DSSCs based on **CBZ**, **WD-5** and **DTA**, and the corresponding data are summarized in Table 3. **CBZ** and **WD-5** sensitized solar cells give short-circuit photocurrent densities (J_{sc}) of 4.25 and 4.45 mA cm^{-2} , open-circuit voltages (V_{oc}) of 586 and 587 mV, and fill factors (ff) of 0.71 and 0.70, corresponding to overall conversion efficiencies (η) of 1.77 and 1.83%, respectively. Under the same condition, the **DTA** sensitized solar cell gives a J_{sc} of 4.78 mA cm^{-2} , a V_{oc} of 608 mV, and an ff of 0.70, corresponding to η of 2.03%. These observations indicate the short-circuit photocurrent as well as the open-circuit voltage increase from **CBZ**, **WD-5** to **DTA**, leading to a linear increment in device efficiency with different electron donors.

According to Fig. 9 and Table 3, it is clear that the photovoltaic performances of the DSSCs can be affected by the different

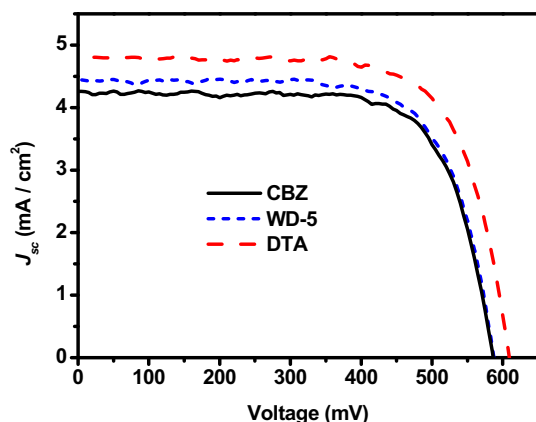


Fig. 9. The J – V curves of DSSCs based on **CBZ**, **WD-5** and **DTA** dyes.

Table 3
Photovoltaic performances of DSSCs based on **CBZ**, **WD-5** and **DTA**.

Dye	$J_{sc}/\text{mA cm}^{-2}$	V_{oc}/mV	ff	η (%)
CBZ	4.25	586	0.71	1.77
WD-5	4.45	587	0.70	1.83
DTA	4.78	608	0.70	2.03

arylamine electron donors in organic dyes. In comparison with **CBZ** and **WD-5**, the photovoltaic performance of **DTA** with the diphenylamine group as electron donor is significantly improved. The higher molar extinction coefficient of **DTA** likely results in a higher J_{sc} value compared with that of **CBZ** and **WD-5**. The higher V_{oc} of **DTA** than those of **CBZ** and **WD-5** might be due to the comparatively more positive HOMO of the former, which offers larger driving force for the reduction of the oxidized dye. This, in turn, will lead to a slower back electron transfer from TiO_2 to the oxidized dye and result in a larger V_{oc} value [22]. The higher J_{sc} and V_{oc} for the device of **DTA** lead to the higher efficiency finally.

3.5. Electrochemical impedance spectroscopy

Electrochemical impedance spectroscopy (EIS) is a useful tool for characterizing important interfacial charge transfer processes in DSSCs, such as the charge recombination at the TiO_2 /dye/electrolyte interface, electron transport in the TiO_2 electrode, electron transfer at the counter electrode, and I_3^- transport in the electrolyte. In this study, EIS analyses were also performed to elucidate the aforementioned photovoltaic findings. This examination was conducted by subjecting the cells to 100 mW cm^{-2} illumination and to bias at the open-circuit voltage (V_{oc}) of the cells.

Fig. 10 shows the EIS Nyquist plots for DSSCs based on **CBZ**, **WD-5** and **DTA**. For the frequency range investigated (0.1 Hz to 100 kHz), a larger semicircle occurs in the lower-frequency range (~ 0.1 Hz to 100 Hz) and a smaller semicircle occurs in the higher-frequency range. With the bias illumination and voltage applied, the larger semicircle at lower frequencies corresponded to the charge transfer processes at the TiO_2 /dye/electrolyte interface, while the smaller semicircle at higher frequencies corresponded to the charge transfer processes at the Pt/electrolyte interface. The two cells showed minimal differences in the smaller semicircles at higher frequencies; however, the difference between the cells in the larger semicircles at lower frequencies was significant. The radius of the lower-frequency semicircle in the Nyquist plot decreased in the following order: **CBZ** > **WD-5** > **DTA**, indicating

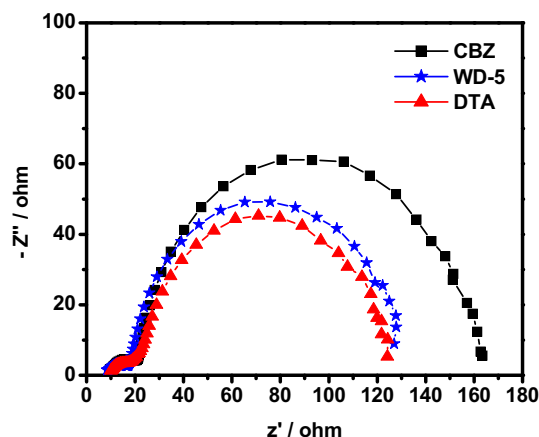


Fig. 10. Nyquist plots for DSSCs sensitized with **CBZ**, **WD-5**, and **DTA** dyes.

that the electron transfer resistance augments from **DTA**, **WD-5** to **CBZ**. The decrease in the lower-frequency semicircle radius with the increase in DSSC efficiency and the smaller radius observed in the higher efficiency **DTA** cell indicate the more efficient electron generation and transport. Thus, the EIS results are in good agreement with results of the short-circuit currents and the overall conversion efficiencies of the DSSCs based on the three dyes.

4. Conclusions

In summary, to further study the effect of different electron donors of organic sensitizers on DSSCs performances, a series of organic sensitizers containing identical π -spacers and electron acceptors but different arylamine electron donors (carbazole, phenothiazine and diphenylamine, respectively) were used in dye-sensitized solar cells. The influence of the different arylamine electron donors on the photophysical, electrochemical properties and photovoltaic performances were studied by spectral, electrochemical, photovoltaic experiments, and density functional theory calculations. Due to the strong electron donating ability of the diphenylamine unit, the **DTA** dye presents the longest maximum absorption wavelength with the highest molar absorption coefficient. The overall conversion efficiency of DSSC based on **DTA** with a diphenylamine unit (2.03%) is higher than those of **WD-5** with a phenothiazine unit (1.83%) and **CBZ** with a carbazole unit (1.77%). Electrochemical impedance spectroscopy results are in good agreement with results of the short-circuit currents and the overall conversion efficiencies of the DSSCs based on the three dyes. These findings reveal that different electron donors in organic sensitizers cause significant differences in photovoltaic performance.

Acknowledgments

We thank the National Natural Science Foundation of China (Grant Nos. 20602005, 20873015), the Fundamental Research Funds for the Central Universities (Grant No. ZYGX2010J035), the Innovation Funds of State Key Laboratory of Electronic Thin Films and Integrated Device (Grant No. CXJJ201104) and Beijing National Laboratory for Molecular Sciences (BNLMS) for financial support.

References

- [1] Chen CY, Wang M, Li JY, Pootrakulchote N, Alibabaei L, Decoppet JD, et al. Highly efficient light-harvesting ruthenium sensitizer for thin-film dye-sensitized solar cells. *ACS Nano* 2009;3:3103–9.

- [2] Seo KD, Song HM, Lee MJ, Pastore M, Anselmi C, Angelis FD, et al. Coumarin dyes containing low-band-gap chromophores for dye-sensitized solar cells. *Dyes and Pigments* 2011;90:304–10.
- [3] Ono T, Yamaguchi T, Arakawa H. Study on dye-sensitized solar cell using novel infrared dye. *Solar Energy Materials & Solar Cells* 2009;93:831–5.
- [4] Matsui M, Kotani M, Kubota Y, Funabiki K, Jin JY, Yoshida T, et al. Comparison of performance between benzoindoline and indoline dyes in zinc oxide dye-sensitized solar cell. *Dyes and Pigments* 2011;91:145–52.
- [5] Matsui M, Fujita T, Kubota Y, Funabiki K, Jin JY, Yoshida T, et al. Substituent effects in a double rhodanine indoline dye on performance of zinc oxide dye-sensitized solar cell. *Dyes and Pigments* 2010;86:143–8.
- [6] Hara K, Sato T, Katoh R, Furube A, Yoshihara T, Murai M, et al. Novel conjugated organic dyes for efficient dye-sensitized solar cells. *Advanced Functional Materials* 2005;15:246–52.
- [7] Chen YS, Li C, Zeng ZH, Wang WB, Wang XS, Zhang BW. Efficient electron injection due to a special adsorbing group's combination of carboxyl and hydroxyl: dye-sensitized solar cells based on new hemicyanine dyes. *Journal of Materials Chemistry* 2005;15:1654–61.
- [8] Im H, Kim S, Park C, Jang SH, Kim CJ, Kim K, et al. High performance organic photosensitizers for dye-sensitized solar cells. *Chemical Communications*; 2010:1335–7.
- [9] Kim D, Lee JK, Kang SO, Ko J. Molecular engineering of organic dyes containing N-aryl carbazole moiety for solar cell. *Tetrahedron* 2007;63:1913–22.
- [10] Zafer C, Gultekin B, Ozsoy C, Tozlu C, Aydin B, Icli S. Carbazole-based organic dye sensitizers for efficient molecular photovoltaics. *Solar Energy Materials & Solar Cells* 2010;94:655–61.
- [11] Wan ZQ, Jia CY, Duan YD, Zhang JQ, Lin Y, Shi Y. Effects of different acceptors in phenothiazine-triphenylamine dyes on the optical, electrochemical, and photovoltaic properties. *Dyes and Pigments* 2012;94:150–5.
- [12] Wu WJ, Yang JB, Hua JL, Tang J, Zhang L, Long YT, et al. Efficient and stable dye-sensitized solar cells based on phenothiazine sensitizers with thiophene units. *Journal of Materials Chemistry* 2010;20:1772–9.
- [13] Tsao MH, Wu TY, Wang HP, Sun IW, Su SG, Lin YC, et al. An efficient metal-free sensitizer for dye-sensitized solar cells. *Materials Letters* 2011;65:583–6.
- [14] Tian HN, Yang XC, Chen RK, Zhang R, Hagfeldt A, Sun LC. Effect of different dye baths and dye-structures on the performance of dye-sensitized solar cells based on triphenylamine dyes. *Journal of Physical Chemistry C* 2008;112:11023–33.
- [15] Wan ZQ, Jia CY, Zhang JQ, Duan YD, Lin Y, Shi Y. Triphenylamine-based starburst dyes with carbazole and phenothiazine antennas for dye-sensitized solar cells. *Journal of Power Sources* 2012;199:426–31.
- [16] Tian HN, Yang XC, Cong JY, Chen RK, Teng C, Liu J, et al. Effect of different electron donating groups on the performance of dye-sensitized solar cells. *Dyes and Pigments* 2010;84:62–8.
- [17] Teng C, Yang XC, Li SF, Cheng M, Hagfeldt A, Wu LZ, et al. Tuning the HOMO energy levels of organic dyes for dye-sensitized solar cells based on Br[−]/Br₃[−] Electrolytes. *Chemistry – A European Journal* 2010;16:13127–38.
- [18] Frisch MJ, Trucks GW, Schlegel HB, Scuseria GE, Robb MA, Cheeseman JR, et al. Gaussian 03, revision C.02. Wallingford, CT: Gaussian Inc.; 2004.
- [19] Liang M, Xu W, Cai FS, Chen PQ, Peng B, Chen J, et al. New triphenylamine-based organic dyes for efficient dye-sensitized solar cells. *Journal of Physical Chemistry C* 2007;111:4465–72.
- [20] Yang CH, Chen HL, Chuang YY, Wu CG, Chen CP, Liao SH, et al. Characteristics of triphenylamine-based dyes with multiple acceptors in application of dye-sensitized solar cells. *Journal of Power Sources* 2009;188:627–34.
- [21] Hagfeldt A, Grätzel M. Light-induced redox reactions in nanocrystalline systems. *Chemical Reviews* 1995;95:49–68.
- [22] Thomas KRJ, Hsu Y, Lin JT, Lee K, Ho K, Lai C, et al. 2,3-disubstituted thiophene-based organic dyes for solar cells. *Chemistry of Materials* 2008;20:1830–40.